



## Excitation of intrinsic localized modes in finite mass-spring chains driven sinusoidally at end

Yosuke Watanabe<sup>a\*</sup>, Takunobu Nishida<sup>a</sup>, and Nobumasa Sugimoto<sup>a,b</sup>

<sup>a</sup> Graduate School of Engineering Science, Osaka University, Toyonaka, Osaka 560-8531, Japan

<sup>b</sup> Faculty of Engineering Science, Kansai University, Suita, Osaka 564-8680, Japan

Received 10 December 2014, accepted 25 June 2015, available online 28 August 2015

**Abstract.** Localized oscillations in finite mass-spring chains, driven sinusoidally at one end with the other fixed, are studied numerically. It is assumed that the restoring force of the spring is given by a piecewise linear function of a relative displacement between neighbouring masses, i.e. a spring constant changes at a threshold of the displacement. Linear damping proportional to the velocity of the mass is taken into account. The mass at one end is forced to be displaced in the direction of the chains at a frequency above the cut-off frequency. It is shown that when the amplitude exceeds the threshold, localized oscillations are excited intermittently at the driving end and propagated down the chain at a constant speed.

**Key words:** nonlinear localized oscillations, intrinsic localized modes, discrete breathers, Fermi–Pasta–Ulam chains, piecewise linear approximation.

### 1. INTRODUCTION

It is known that the intrinsic localized modes (ILMs) or the discrete breathers (DBs) are generic in spatially periodic, discrete, and nonlinear systems (see, for example [1–5]). It is also known that the mobile type of ILMs can be excited both in a spatially infinite system [6] and a semi-infinite system driven at one end sinusoidally at a frequency in a linear stopping band above the passing band [7–11]. However, most of the works are theoretical ones and, to the best of our knowledge, only a few works are concerned experimentally with the ILMs (for example [12–14]). This paper considers motions of finite mass-spring chains driven sinusoidally at one end with the other fixed, and show existence of the ILMs numerically, aiming at experimental demonstration of them. Our model assumes that the restoring force of the spring is given by a piecewise linear function of a relative displacement of neighbouring masses, i.e. the spring constant changes at a threshold of the displacement.

Such a chain may be compared with the celebrated Fermi–Pasta–Ulam (FPU) chains as a paradigm of the ILMs where the restoring force is given by a cubic function of displacement called the FPU- $\beta$  model [15]. Our model has similarity and also dissimilarity with the FPU- $\beta$  model. The piecewise linear spring behaves similarly to the cubic spring when the displacement is comparable with the threshold. However, when the displacement is far beyond the threshold, the piecewise linear spring is linear, not nonlinear, roughly speaking. On the other hand, the FPU- $\beta$  chains are infinite without ends and no external excitation is considered. Thus our model is different from the FPU- $\beta$  model, nevertheless, it is shown that the ILMs emerge commonly.

---

\* Corresponding author, [watanabe@me.es.osaka-u.ac.jp](mailto:watanabe@me.es.osaka-u.ac.jp)

So far no experiments of the ILMs have ever been done on the FPU- $\beta$  model. One of the reasons behind the lack of experiments is speculated to be unavailability of appropriate cubic springs. This prompts us to consider the piecewise linear spring. In order to find suitable masses and springs to be used, simulations are done in the first place. The system of finite chains is solved numerically by exciting one end of the chains sinusoidally with the other fixed. The model includes a small, linear damping proportional to velocity, which is unavoidable in experiments. It is expected by the results of simulations that the ILMs can be excited experimentally as well.

## 2. NUMERICAL ANALYSIS

Chains' motions are described by the following set of equations for  $N(\gg 1)$  masses given by

$$m\ddot{x}_j = F(r_j) - F(r_{j-1}) + c(\dot{r}_j - \dot{r}_{j-1}), \quad (1)$$

with boundary conditions

$$x_0(t) = A \sin \omega_d t \quad \text{and} \quad x_{N+1}(t) = 0, \quad (2)$$

where  $x_j$  ( $j = 1, \dots, N$ ) represent positions of the  $j$ th mass along the chains from the equilibrium point and  $r_j = x_{j+1} - x_j$ ;  $c$  is a damping coefficient, while  $A$  and  $\omega_d$  are a driving amplitude and angular frequency, respectively. Let the function  $F(r)$  be composed of three linear functions with the inclination  $k_L$  for small displacement, and  $k_{\text{push}}$  and  $k_{\text{pull}}$  for larger displacement  $r \leq r_{\text{push}}$  and  $r \geq r_{\text{pull}}$ , respectively, where  $r_{\text{push}} (< 0)$  and  $r_{\text{pull}} (> 0)$  give the thresholds on  $r$ , where the spring constants change as follows:

$$F(r) = \begin{cases} k_{\text{push}} r + (k_L - k_{\text{push}}) r_{\text{push}}, & (r \leq r_{\text{push}}), \\ k_L r, & (r_{\text{push}} \leq r \leq r_{\text{pull}}), \\ k_{\text{pull}} r + (k_L - k_{\text{pull}}) r_{\text{pull}}, & (r_{\text{pull}} \leq r). \end{cases} \quad (3)$$

If  $k_{\text{pull}}$  is equal to  $k_{\text{push}}$ ,  $F(r)$  is antisymmetric with respect to the equilibrium point. For reference, the FPU- $\beta$  model takes  $F(r)$  in the form of  $F(r) = k_L r + k_C r^3$ ,  $k_L$  and  $k_C$  being constant. A piecewise linear function is compared in Fig. 1 with a cubic function for appropriate values for parameters.

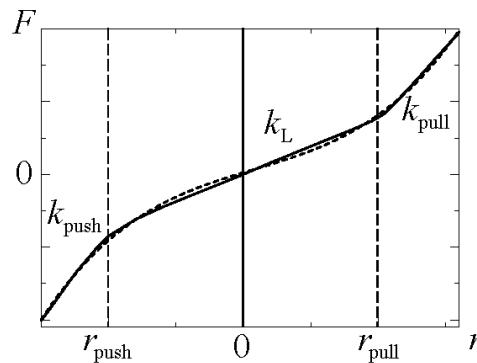


**Fig. 1.** Piecewise linear function (3) by the solid line and the cubic function to the FPU- $\beta$  model by the broken line, which are antisymmetric with respect to the equilibrium point.

For the finite chains of 39 masses except for those at both ends, numerical values of the parameters are chosen as follows:  $m = 99.1 \times 10^{-3}$  kg,  $c = 2.12 \times 10^{-3}$  Ns/m,  $k_L = 39.2$  N/m,  $k_{\text{push}} = 118$  N/m,  $k_{\text{pull}} = 99.1$  N/m, and  $r_{\text{pull}} = -r_{\text{push}} = 20.0 \times 10^{-3}$  m. The values  $k_L$ ,  $k_{\text{push}}$ ,  $k_{\text{pull}}$ ,  $r_{\text{pull}}$ , and  $r_{\text{push}}$  are determined by the measurements of springs to be used in experiments. Because  $k_{\text{pull}}$  differs a little from  $k_{\text{push}}$ , the spring is not antisymmetric exactly. Details on the springs are not described here.

As is well known, there are  $N$  eigenfrequencies  $\omega_n$  ( $n = 1, \dots, N$ ) in the linearized system given by

$$\omega_n = 2\sqrt{\frac{k_L}{m}} \sin \frac{n\pi}{2(N+1)}, \quad (4)$$

and they lie below the limit value  $\omega_\infty = 2\sqrt{k_L/m}$  [15]. For the present chains, the cut-off angular frequency is calculated to be  $\omega_{39} = 39.8$  rad/s. The driving angular frequency  $\omega_d$  is taken to be slightly higher than the cut-off one,  $\omega_d = 41.5$  rad/s.

Letting one end at  $x_0$  be driven from a quiescent state sinusoidally at a frequency above the cut-off one, we solve Eq (1) with the boundary conditions (2) by the Runge–Kutta method. It is found numerically that while the driving amplitude is below the threshold, the oscillations are evanescent and confined near the end (Fig. 2). Small ripples are seen because the impulse at  $t = 0$  excites various frequency modes. As the driving amplitude is increased beyond the threshold, the localized oscillations are excited intermittently at the driving end and propagated down the system at a constant speed (Fig. 3).

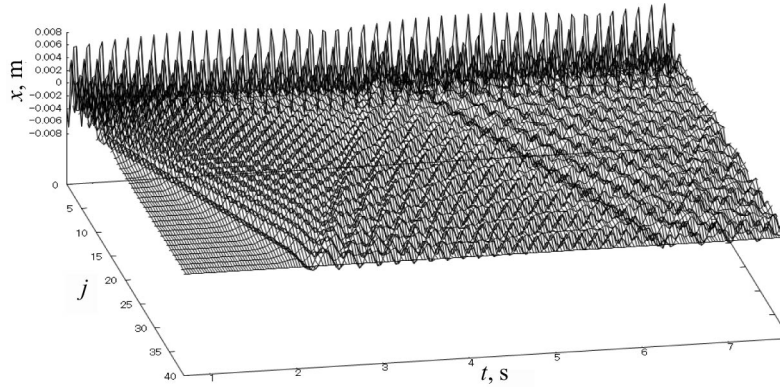


**Fig. 2.** Spatial and temporal profile of the positions of the masses from the quiescent state for the small driving amplitude  $A = 7.00 \times 10^{-3}$  m below the threshold. Excitations are confined near the driver end due to the evanescent oscillations.

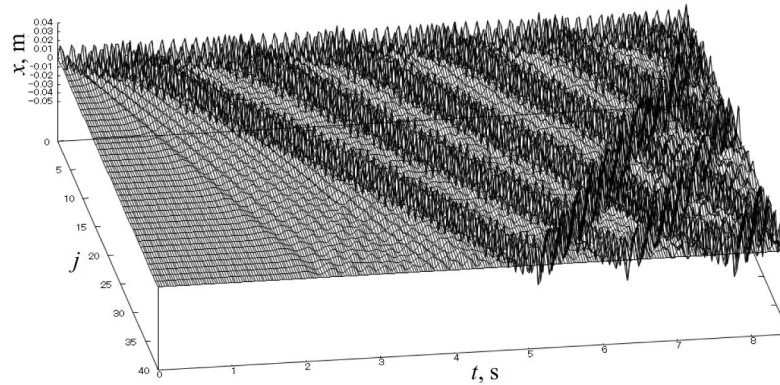


**Fig. 3.** Spatial and temporal profile of the positions of the masses from the quiescent state for the larger driving amplitude  $A = 15.0 \times 10^{-3}$  m beyond the threshold. The ILMs are excited intermittently at the driving end and propagated down the system.

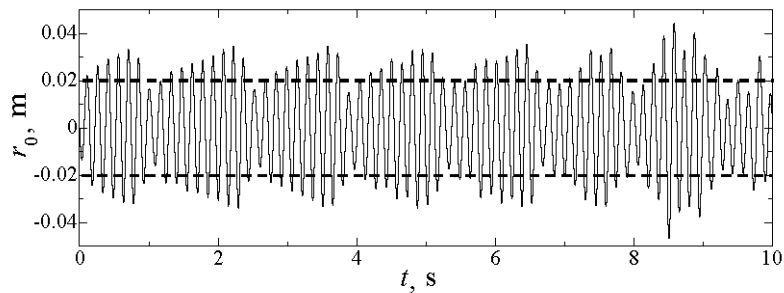


**Fig. 4.** Temporal profile of the relative displacement  $r_0 (= x_1 - A \sin \omega_d t)$ . When the amplitude exceeds the threshold, the localized oscillations are excited by the driving amplitude  $A = 15.0 \times 10^{-3}$  m.

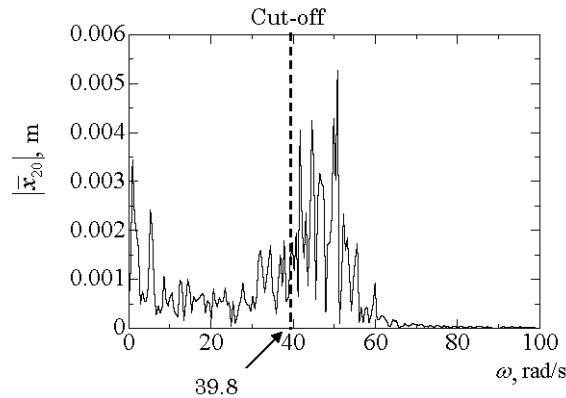


**Fig. 5.** Frequency spectrum  $|\bar{x}_{20}|$  of the oscillations of the 20th mass in Fig. 3. The oscillations are seen to consist of the nonlinear modes of localized oscillations and linear modes initially excited at driven end.

Figure 4 shows the temporal profile of  $r_0$  for the displacement of spring adjacent to the driver at the driving amplitude  $A = 15.0 \times 10^{-3}$  m. The localized oscillations are excited when  $|r_0|$  exceeds the threshold  $A = 20.0 \times 10^{-3}$  m in Fig. 4. When the localized oscillations hit the other end, they are reflected and propagated back in the system, subject to nonlinear interactions between them, and with the driving end. The FFTs show that the highest peak of the oscillations is located in the linear stopping band (Fig. 5). In these respects, the oscillations may be regarded as the moving ILMs.

However, as the driving amplitude exceeds far beyond the threshold, the ILMs do not tend to be formed but to be evanescent. This is because the chains behave linearly so that the cut-off frequency is shifted to  $2\sqrt{k_{\text{push}}(\text{pull})/m}$ , beyond which the evanescent mode revives.

### 3. CONCLUSIONS AND REMARKS

Excitation and propagation of the moving ILMs have been shown numerically in the finite mass-spring chains with the piecewise linear springs driven sinusoidally at one end with the other fixed. It has been revealed that the ILMs are generated when the relative displacement of the mass next to the driving end exceeds the threshold one at which the spring constant changes. The relation between the driving amplitude and frequency to excite ILMs is similar to the one for the ILMs in the case of the FPU- $\beta$  model unless the amplitude is too large. The present results are used to implement the experiments of the ILMs, and results of the experiments will be published in a forthcoming paper.

## ACKNOWLEDGEMENTS

The authors thank Dr K. Yoshimura for useful comments. This work was supported by JSPS KAKENHI grant Nos 24654124 and 26400394.

## REFERENCES

1. Sievers, A. J. and Takeno, S. Intrinsic localized modes in anharmonic crystals. *Phys. Rev. Lett.*, 1988, **61**(8), 970–973.
2. Aubry, S. Breathers in nonlinear lattices: existence, linear stability and quantization. *Physica D*, 1997, **103**, 201–250.
3. Flach, S. and Willis, C. R. Discrete breathers. *Phys. Rep.*, 1998, **295**, 181–264.
4. Kivshar, Y. S. and Flach, S. (eds). Focus issue: Nonlinear localized modes: physics and applications. *Chaos*, 2003, **13**, 586–799.
5. Campbell, D. K., Flach, S., and Kivshar, Y. S. Localizing energy through nonlinearity and discreteness. *Phys. Today*, 2004, **57**, 43–49.
6. Yoshimura, K. and Doi, Y. Moving discrete breathers in nonlinear lattice: resonance and stability. *Wave Motion*, 2007, **45**, 83–99.
7. Geniet, F. and Leon, J. Energy transmission in the forbidden band gap of a nonlinear chain. *Phys. Rev. Lett.*, 2002, **89**(13), 134102.
8. Geniet, F. and Leon, J. Nonlinear supratransmission. *J. Phys.-Condens. Mat.*, 2003, **15**, 2933–2949.
9. Spire, A. and Leon, J. Nonlinear absorption in discrete systems. *J. Phys. A-Math. Gen.*, 2004, **37**, 9101–9108.
10. Leon, J. Nonlinear supratransmission as a fundamental instability. *Phys. Lett. A*, 2003, **319**, 130–136.
11. Khomeriki, R., Lepri, S., and Ruffo, S. Nonlinear supratransmission and bistability in the Fermi-Pasta-Ulam model. *Phys. Rev. E*, 2004, **70**, 066626.
12. Sato, M., Hubbard, B. E., Sievers, A. J., Ilic, B., Czaplowski, D. A., and Craighead, H. G. Observation of locked intrinsic localized vibrational modes in a micromechanical oscillator array. *Phys. Rev. Lett.*, 2003, **90**, 044102.
13. Kimura, M. and Hikiyama, T. Coupled cantilever array with tunable on-site nonlinearity and observation of localized oscillations. *Phys. Lett. A*, 2009, **373**, 1257–1260.
14. Cuevas, J., English, L. Q., Kevrekidis, P. G., and Anderson, M. Discrete breathers in a forced-damped array of coupled pendula: modeling, computation, and experiment. *Phys. Rev. Lett.*, 2009, **102**, 224101.
15. Gallavotti, G. (ed.). *The Fermi-Pasta-Ulam Problem*. Springer, Berlin, Heidelberg, 2008.

## Mass-vedru tüüpi lõpliku ahela loomulike võnkemoodide sinusoidaalne ergastamine

Yosuke Watanabe, Takunobu Nishida ja Nobumasa Sugimoto

On uuritud numbriliselt mass-vedru tüüpi lõpliku ahela lokaalseid võnkumisi. Ahela üks ots on fikseeritud ja teises mõjub sinusoidaalne jõud. Vedrus mõjuva jõu ja naabermasside relatiivse siirde vahelist mittelineaarset seost aproksimeeritakse tükati lineaarse funktsiooniga. Arvesse on võetud lineaarset sumbuust, mis on proportsionaalne massi kiirusega. Ahela vabas otsas olevat massi liigutatakse ahelasihiliselt sinusoidaalse jõuga, mille sagedus on piirsagedusest kõrgem. On näidatud, et kui amplituud ületab teatava läve, siis lokaalsed võnkumised ergastuvad alates vabast otsast (kus mõjub perioodiline jõud) ja et ergastus liigub mööda ahelat jääva kiirusega.